ELSEVIER

Journal of Organometallic Chemistry 555 (1998) 167–175

Journal of Organometallic Chemistry

The transition-metal complexes of the thiamacrocycle containing two ferrocene nuclei in the main chain. Synthesis, properties, and molecular structure of Ag(I), Cu(I), Pd(II), and Pt(II) complexes of 1,5,16,21-tetrathia[5.5]ferrocenophane

Masaru Sato *, Hirofumi Anano

Chemical Analysis Center, Saitama University, Urawa, Saitama 338, Japan

Received 29 July 1997; received in revised form 21 September 1997

Abstract

1,5,16,21-Tetrathia[5.5]ferrocenophane reacted with $(MeCN)_4CuClO_4$ and $AgBF_4$ in THF to give the 1:1 complexes in good yields. The treatment of the ligand with $(MeCN)_2MCl_2$ (M = Pd and Pt) and two equivalents of $AgBF_4$ in MeCN gave the 1:1 complexes in good yields. A reversible two-electron redox wave was observed near + 0.3 V in the Cu(I) and Ag(I) complexes. The Pd(II) and Pt(II) complexes showed the irreversible two-electron oxidation wave near + 0.7 V and that of the Pd(II) complex exhibited a slight peak separation, inferring a small interaction between the two Fe atoms through the central Pd(II) atom. As can be seen by X-ray analysis, the free ligand employed the pseudo-square conformation with regard to the thiamacrocycle in the molecular structure. The Pt(II) complex took the square-planar arrangement around the Pt(II) atom, while the Cu(I) and Ag(I) complexes maintained the tetrahedral configuration around the metal center.

Keywords: Thiamacrocycle; Ferrocene; Transition-metal complexes

1. Introduction

Transition-metal complexes with thioether ligands have much current interest from the viewpoint of coordination chemistry and biological aspects. Such complexes have been extensively reviewed [1–3]. Of particular interest in coordination and organometallic chemistry are metal complexes of macrocyclic polythioether in which an additional transition metal is contained in the main chain [4,5]. These organometallic ligands are a useful starting material for preparing heterobimetallic complexes, for which a modified catalytic activity, a unique reactivity, and a unique functionality, etc. are expecting. We previously reported the transition metal complexes of polythia[*n*]ferrocenophanes, such an organometallic ligand [6–10]. In the Pd(II) or Pt(II) complex of trithia[*n*]ferrocenophane ($n = 7$ or 9), a strong bonding interaction was observed between two metal sites [10]. The thiamacrocycle condensed with two ferrocenes is interesting from the viewpoint of the investigation about metal–metal interaction. We here report the synthesis, electrochemical properties, and molecular structure of 1,5,16,20-tetrathia[5.5]ferrocenophane and its transition metal complexes.

2. Results and discussion

A solution of disodium ferrocene-1,1′-dithiolate in ethanol and a solution of 1,1′-bis(3-chloropropylthio)ferrocene [11] in THF were added at the same rate and slowly into a large amount of refluxing ethanol. After the usual work-up, 1,5,16,20-tetrathia[5.5]ferrocenophane (**1**)

* Corresponding author.

0022-328X/98/$19.00
PII S0022-328X(97)00682-7

Table 1
Crystal and intensity collection data for **1–4**

	1	**2**	**3**	**4**
Formula	$C_{26}H_{28}S_4Fe_2$	$C_{26}H_{28}BF_4S_4Fe_2Ag$	$C_{28}H_{32}Cl_3O_4S_4Fe_2Cu$	$C_{26}H_{28}B_2F_8S_4Fe_2Pt$
F_w	580.50	775.10	842.40	949.15
System	Monoclinic	Triclinic	Triclinic	Orthorhombic
Space group	$P2_1/n$	$P\bar{1}$	$P\bar{1}$	$Pc2_1/n$
a, Å	8.968(3)	11.347(2)	11.024(4)	9.995(1)
b, Å	11.797(4)	11.849(5)	12.480(3)	12.025(2)
c, Å	12.535(6)	12.025(8)	14.698(5)	27.26(1)
α, deg		62.66(3)	105.04(2)	
β, deg	111.00(3)	81.68(3)	93.17(1)	
γ, deg		81.87(3)	107.02(2)	
V, Å^3	1238.0(8)	1415.7(1)	1848.4(1)	3275.9(0)
Z	2	2	2	4
D_{calc}, g cm^{-3}	1.994	1.818	1.513	1.924
Crystal dimensions, mm^3	$0.2\times0.2\times0.12$	$0.36\times0.30\times0.22$	$0.2\times0.1\times0.05$	$0.4\times0.2\times0.12$
Radiation (λ, Å)	0.71073	0.71073	0.71073	0.71073
Reflection (hkl) limits	$-11<h<10,-15<k<0,$ $0<l<16$	$-14<h<14,-15<k<13,$ $-15<l<0$	$0<h<14,-16<k<14,$ $-20<l<20$	$0<h<13,0<k<17,$ $0<l<38$
Total reflections measured	3223	7026	7139	4688
Unique reflections	2682	6175	2273	3869
Linear absorption coefficient, cm^{-1}	15.096	20.167	18.127	54.87
Reflections used in LS	2281	5623	2273	3869
LS parameters	201	418	379	387
R	0.038	0.053	0.130	0.047
R_w	0.045	0.071	0.168	0.061
Max peak in final Fourier map, e Å^{-3}	0.71	0.85	4.30	3.53
Min peak in final Fourier map, e Å^{-3}	−0.62	−1.00	−0.89	−0.99

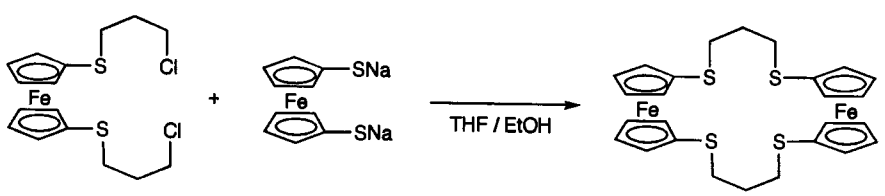

1

was obtained as orange crystals with a 40% yield. The ^{1}H-NMR spectrum of **1** showed a sharp singlet at δ 4.29 (16H), a triplet at δ 3.03 (8H), and a quintet at δ 1.88 (4H), indicating the free rotation of the molecule in liquid state. In order to obtain the information about the molecular structure in solid state, the single crystal X-ray diffraction of **1** was carried out. The crystallographic data of **1** are summarized in Table 1 and selected bond distance, bond angles, and torsion angles are collected in Table 2. The ORTEP view of **1** is shown in Fig. 1. The thiamacrocycle in **1** adopts a pseudo-square conformation [3] with two S atoms at a corner and two S atoms in side positions and is different from that of [20]aneS_4 which has a similar ring-size of the thiamacrocycle and four S atoms at a corner [12,13]. Four S–C(sp^3) bonds and four C(sp^3)–C(sp^3) bonds in **1** lie in gauche placements and the Cp rings of the ferrocene nuclei adopt a staggered conformation. As the result, the compound **1** adopts *exo* conformation with the S-donors pointing out of the macrocyclic cavity. Rearrangement from an *exo* to *endo* conformation would be, therefore, required in the coordination chemistry of **1**.

When a solution of $AgBF_4$ in THF was added to a solution of **1** in THF, yellow crystals precipitated immediately. The crystals were identified as the 1:1 complex

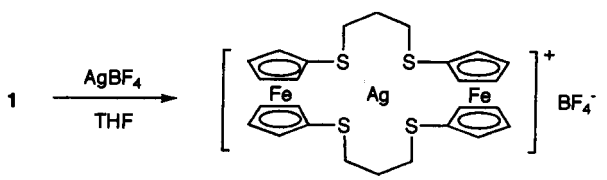

2

of **1** with $AgBF_4$ by elemental analysis. The ^{1}H-NMR spectrum of **2** gave sharp signals which consisted of a

Table 2
Selective bond distances, bond angles and torsion angles of 1

Bond distances (Å)			
C(1)–S(1)	1.757(5)	C(6)–S(2)	1.768(4)
C(11)–S(1)	1.824(5)	C(13)–S(2)	1.828(5)
Fe(1)–C	2.049(av.)	C–C (ring)	1.426(av.)
Bond angles (°)			
C(1)–S(1)–C(11)	101.9(3)	C(6)–S(2)–C(13)	99.4(2)
S(1)–C(11)–C(12)	108.6(4)	S(2)–C(13)–C(12)	113.8(4)
Torsion angles (°)			
C(1)–S(1)–C(11)–C(12)		−175.1(4)	
S(1)–C(11)–C(12)–C(13)		68.0(4)	
C(11)–C(12)–C(13)–S(2)		62.5(4)	
C(12)–C(13)–S(2)–C(6)		53.7(4)	

Table 3
Selective bond distances and bond angles of 2

Bond distances (Å)			
Ag(1)–S(1)	2.618(2)	Ag(1)–S(2)	2.641(3)
Ag(1)–S(3)	2.589(2)	Ag(1)–S(4)	2.595(3)
C(1)–S(1)	1.761(7)	C(6)–S(4)	1.765(7)
C(11)–S(2)	1.758(8)	C(16)–S(3)	1.765(9)
C(21)–S(1)	1.831(9)	C(23)–S(2)	1.839(9)
C(24)–S(3)	1.824(11)	C(26)–S(4)	1.869(11)
Fe(1)–C	2.054(av.)	C–C (ring)	1.438 (av.)
Bond angles (°)			
S(1)–Ag(1)–S(2)	90.8(1)	S(1)–Ag(1)–S(4)	108.8(1)
S(2)–Ag(1)–S(3)	103.9(1)	S(3)–Ag(1)–S(4)	92.6(1)
S(1)–Ag(1)–S(3)	144.9(1)	S(2)–Ag(1)–S(4)	117.5(1)
C(1)–S(1)–C(21)	99.9(4)	C(11)–S(2)–C(23)	99.9(4)
C(16)–S(3)–C(24)	100.7(5)	C(6)–S(4)–C(26)	99.4(4)
S(1)–C(21)–C(22)	118.3(6)	S(2)–C(23)–C(22)	111.8(6)
S(3)–C(24)–C(25)	118.3(8)	S(4)–C(26)–C(25)	111.5(8)

double doublet at δ 4.51 (16H), a triplet at δ 3.06 (8H), and a quintet at δ 2.02 (4H), suggesting that complex **2** enjoys a free motion in the solution at the time-scale of NMR. The Cp ring protons in the ferrocene nuclei and the methylene protons next to the S atoms were shifted down-field slightly. The tiny down-field shift may suggest the weak coordination bond between the S atom and the central Ag(I) ion. This seems to be supported by the crystal structure of **2**.

Yellow crystals of **2**, suitable for X-ray structure analysis, could be grown from MeCN/diethylether by the slow diffusion method. The crystallographic data are listed in Table 1 and the selected bond distances and bond angles are summarized in Table 3. An ORTEP presentation of the complex cation is given in Fig. 2. The structure exhibits the Ag(I) center in strongly distorted tetrahedral coordination geometry. Those structural features seem to be a result of the compromise between the maintenance of the conformation in the free ligand **1** and the conformational rearrangement from the *exo*- to *endo*-conformation with regard to the S atoms by the coordination to the Ag atom. To our knowledge, this is the first example of the tetrahedral Ag(I) complex of the 4S-containing thiamacrocycle. The Ag–C bond distances are not abnormal because

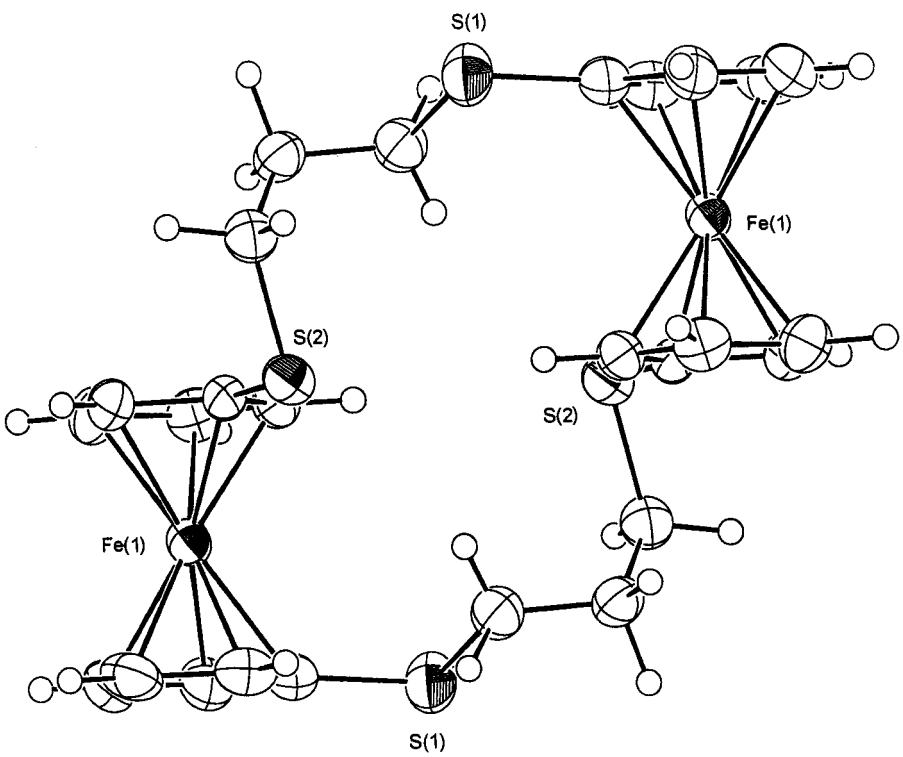

Fig. 1. ORTEP view of **1**.

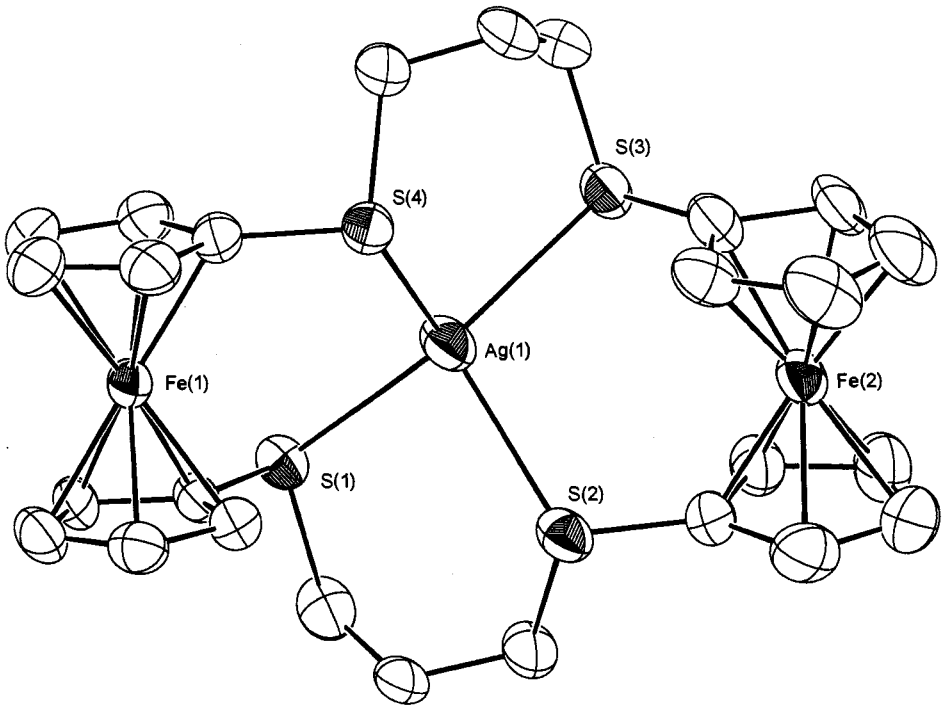

Fig. 2. ORTEP view of the cationic part of **2**.

they resemble the typical value of ≈2.60 Å and are different from the long distances observed in [Ag(9-aneS$_3$)$_2$][CF$_3$SO$_3$] which range from 2.696(2) to 2.753(1) Å [14]. Detailed analysis of the bond lengths reveals that the distance of two Ag–C bonds is somewhat long [Ag–S(1) = 2.618(2) and Ag–S(2) = 2.641(3) Å] and that of the other two bonds is short [Ag–S(3) = 2.589(2) and Ag–S(4) = 2.595(3) Å]. The behavior is similar to those observed in [Ag([19]aneS$_6$–OH)][CF$_3$SO$_3$] which has a distorted tetrahedral arrangement around the Ag(I) atom [15]. Strong deviations from the ideal tetrahedral angle are observed: two compressed angles of 90.8(1) [S(l)–Ag–S(2)] and 92.6(1)° [S(3)Ag–S(4)] and two enlarged angles 108.8(1) [S(1)–Ag–S(4)] and 103.9(1)° [S(2)–Ag–S(3)]. It is worthy to note that the 1,1′-ferrocenylene group is bonded to the S atoms which forms the latter angles. The enlarged angles observed are probably because the distance between the S atoms is compelled by the inter-ring distance (3.3 Å) of ferrocene. A similar and slightly large deviation is also observed in [Ag([19]aneS$_6$–OH)][CF$_3$SO$_3$] [15]. The Ag(1)–Fe(1) and Ag(1)–Fe(2) distances are 4.105(2) and 4.193(2) Å, respectively. These are longer by ca. 0.1 Å than that in the Pt(II) complex (see below), being probably due to the larger atomic radius of the Ag atom (1.44 Å), compared with that of the Pt atom (1.38 Å) and the configurational difference around the metal.

Compound **1** was treated with Cu(BF$_4$)$_2$·xH$_2$O–Ac$_2$O in nitromethane but no definite complex was obtained, while the reaction of **1** with Cu(MeCN)$_4$ClO$_4$ in MeCN–THF gave the 1:1 complex (**3**) as yellow needles in 73% yield. The ^{1}H-NMR spectrum of

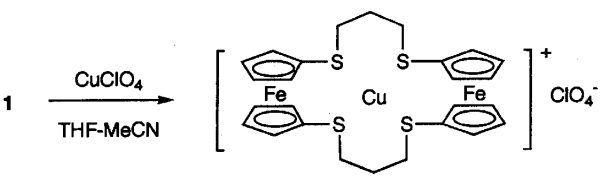

3

showed broad singlets at δ 2.05 (4H), 3.27 (8H), 4.52 (8H) and 4.62 (8H). The somewhat broadening of the signals observed may be due to a slight appearance of a paramagnetic species in highly polar solvent, CD$_3$NO$_2$. The larger down-field shift of all signals and the increased splitting of the α- and β-ring proton of the ferrocene nucleus (Δ 0.10 ppm), compared with those of the free ligand and the Ag(I) complex (**2**), suggest that there may be a certain interaction between the Fe atom of the ferrocene nucleus and the central Cu(I) atom. Orange/red X-ray quality crystals of **3** were obtained by recrystallization from dichloroethane. The crystallographic data are summarized in Table 1 and the structure of the cation part is shown in Fig. 3. The crystals contained a molecule of dichloroethane in the crystal lattice. The detailed discussion about the bond distance

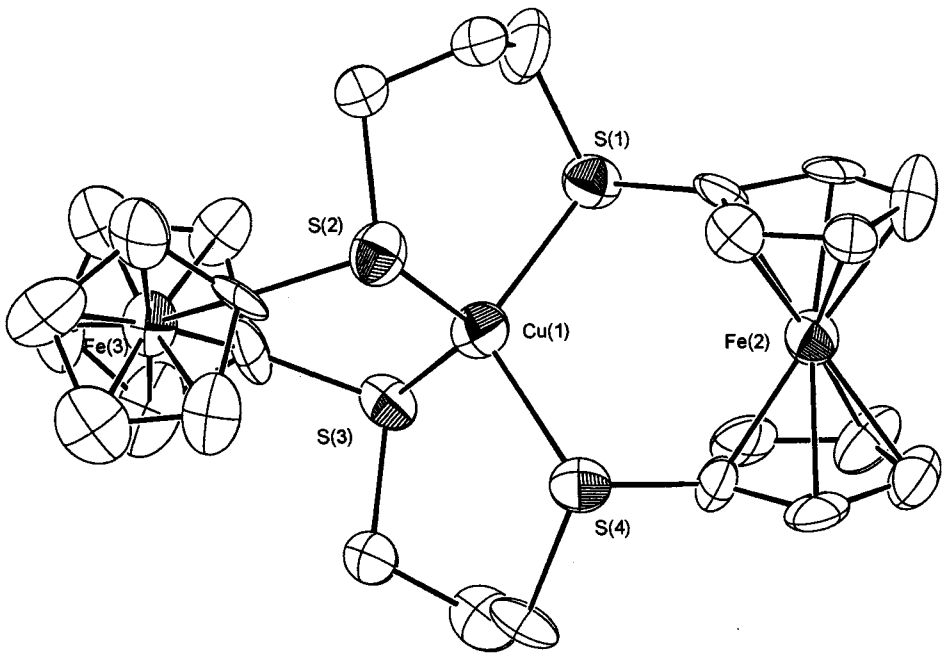

Fig. 3. ORTEP view of the cationic part of **3**.

and bond angle in **3** may be meaningless because of an unsatisfactory R value ($R = 0.13$), but the molecular geometry of **3** is clearly understood. The Cu(I) atom incorporated in the tetrathiamacrocycle of **3** takes a little distorted tetrahedral arrangement [S(1)–Cu–S(2) 105.0(5), S(2)–Cu–S(3) 120.3(5), S(3)–Cu–S(4) 104.9(5), S(1)–Cu–S(4) 114.9(5)]. The adoption of this arrangement is coincident to a strong tendency of the Cu(I) atoms to achieve a tetrahedral geometry [16] and the degree of the distortion from the tetrahedron in **3** is much smaller than that in the Ag(I) complex **2**, although the strain in **3** seems to be larger than that in **2** because of shorter Cu–S distances due to the small radius of the Cu atom (1.28 Å). The one ferrocene nucleus is arranged in almost parallel (2°) or a little twisted (12°) towards the other ferrocene nucleus in the free ligand **1** and the Ag complex **2**, respectively, while the two ferrocene nuclei are twisted each other almost perpendicularly (76°). This also indicates that a Cu(I) ion prefers strongly a tetrahedral arrangement.

When the thiacrown ether **1** was treated with $(MeCN)_4Pt(BF_4)_2$, prepared from the reaction of $(MeCN)_2PtCl_2$ with two equivalents of $AgBF_4$ in MeCN, the 1:1 complex

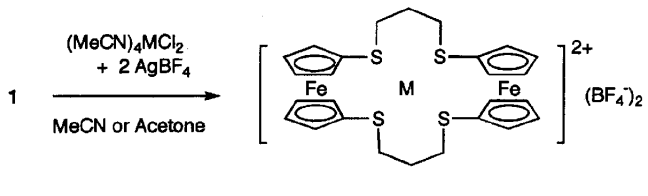

4 M = Pt
5 M = Pd

was obtained as red/orange crystals in good yield. In a similar manner, the green Pd(II) analog (**5**) was prepared. Complex **4** showed a fractional behavior in the ^{1}H-NMR spectrum. That is, the signals of the Cp ring-protons at δ 5.25 (4H) and 4.71 (4H) and the protons neighboring the S atoms at δ 3.09 were broadened at room temperature. In the VT-NMR experiment of **4** the α- and β-protons of the ferrocene part were coalesced at -14 and $+2$°C, respectively, and the fixed spectrum was obtained at -40°C, while the averaged spectrum was obtained at $+55$°C. The similar fluxionality is also observed in the Pt(II) complexes of tetrathia[n](1,1′)ferrocenophanes ([9]b). Interestingly, the coalescence temperature (T_c) of **4** (2°C) is lower than that of the Pt(II) complex of 1,5,9,13-tetrathia[13]ferrocenophane (50°C) which is considered to have less steric strain. At low temperature (-40°C), two pairs of four signals assignable to the ring protons of ferrocene (the ratio of the signal intensity was ca. 2:1) were observed (see Section 3). This indicates that two conformational isomers are fixed in the cold solution. In the fixed spectrum of **4**, the methylene protons next to the S atom in the major isomer appeared at δ 3.09 as a triplet ($J = 13$ Hz) and δ 2.67 as a double doublet ($J = 13$ and 4 Hz) and those in the minor isomer were observed at δ 3.29 and 2.98 as multiplets which were assignable using the H,H-COSY method at -40°C. On the consideration of the molecular model, the major isomer is identified to be the *syn*-isomer which the two ferrocene parts are located in the same side of a planar thiamacrocycle containing the Pt(II) atom and its structure is the same with the crystal

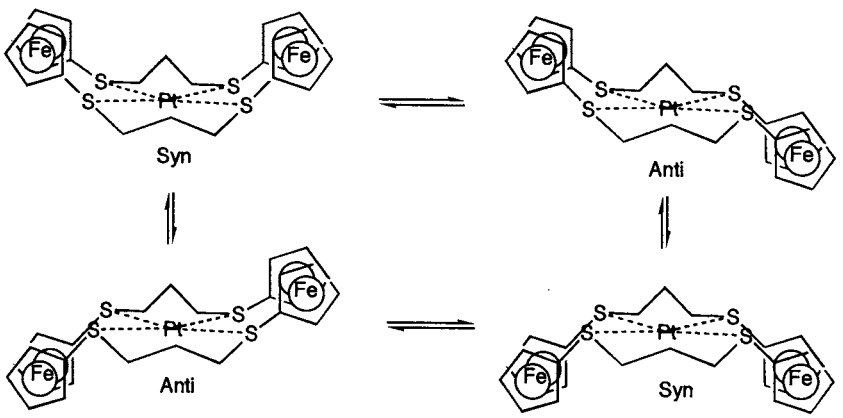

Scheme 1. Complex **4** demonstrating a flipping motion (a simultaneous inversion at two S atoms) between the *syn*- and *anti*-isomers.

structure of **4** (see below). Therefore, the dynamic behavior observed seems to be due to a flipping motion (a simultaneous inversion at two S atoms) between the *syn*- and *anti*-isomers as shown in Scheme 1, although the flipping motion of the central methylene group in the trimethylene-chain parts is also possible. The latter possibility may be excluded by the largely different chemical shift of the β- and β'-ring protons (Δ 0.27 ppm in the major isomer and Δ 0.24 ppm in the minor isomer) in the two fixed conformers at low temperature (the assignment of the α- and β-protons of the ferrocene ring is based on the H,H-COSY spectrum, Scheme 1).

The large down-field shift (Δ 0.95 and 0.44 ppm) and splitting (Δ 0.54 ppm) of the α- and β-protons of the ferrocene ring imply that there is a strong interaction between the ferrocene nucleus and the central Pt(II) atom in the thiamacrocycle. The interaction seems probably due to an inductive or field effect which stems from the strong Lewis-acidity of the Pt(II) atom [17] compared with that of the Cu(I) or Ag(I) atom, because the Fe–Pt dative bond is impossible (see below). A similar fluxional behavior and structural features were also observed in the VT-NMR spectrum of the Pd(II) complex **5**. The averaged spectrum was obtained above 35°C and the coalescence temperature was -25°C for the β-protons of the ferrocene ring. The fact that the Pd(II) complex is more flexible is also observed in the Pd(II) ($T_c = 42$°C) and Pt(II) complexes ($T_c = 50$°C) of 1,5,9,13-tetrathia[13]ferrocenophane ([9]a,b).

The single-crystal X-ray analysis of complex **4** was successful. The crystallographic data are collected in Table 1 and the selected bond distances, angles, and torsion angles are summarized in Table 4. The ORTEP view of the cation structure of **4** is shown in Fig. 4. The coordination mode around the Pt(II) atom was a slightly distorted square-planar arrangement. The S(2)–Pt–S(3) and S(1)–Pt–S(4) angles (~ 81°) holding the ferrocene nucleus were smaller than the S(1)–Pt–S(2) and S(3)–Pt–S(4) angles (~ 98°) holding the trimethylene chain. This may reflect the small S(1)–S(4) and S(2)–S(3) distance constrained by the interring distance of ferrocene (3.32 Å). One of the most remarkable features is the *syn*-arrangement of two ferrocene moieties. The planes S(1)–C(1)–C(6)–S(4) and S(2)–C(11)–C(16)–S(3) are folded in the same side of the tetrathiamacrocycle involving the Pt(II) atom by 60.54(3) and $-60.36(3)$°, respectively. These are considerably smaller than the similar folding angle (83.82°) observed in the Pd(II) complex of 1,5,9,13-tetrathia[13]ferrocenophane which has a similar ring-size to the thiamacrocycle [18]. The Fe–Pt distances in **4** were 3.996(2) and 4.004(3) Å, which were fairly longer than that (3.729(2) Å) of the analogous Pd(II) complex of 1,5,9,13-tetrathia[l3]ferrocenophane. This seems to be due to the smaller folding angle in **4** compared with that in the latter complex since the atomic radius of the Pd (1.37 Å) and Pt atoms (1.38 Å) is similar.

The electrochemical property of complexes **2**–**5** was examined by the cyclic voltammetry. Their redox potentials are summarized in Table 5 and the cyclic voltammogram of **5** is shown in Fig. 5. In the Ag(I) (**2**)

Table 4
Selective bond distances and bond angles of 4

Bond distances (Å)			
Pt(1)–S(1)	2.302(12)	Pt(1)–S(2)	2.304(11)
Pt(1)–S(3)	2.353(12)	Pt(1)–S(4)	2.346(12)
C(1)–S(1)	1.80(3)	C(11)–S(2)	1.68(4)
C(16)–S(3)	1.82(4)	C(6)–S(4)	1.83(4)
C(21)–S(1)	1.83(5)	C(23)–S(2)	1.99(4)
C(24)–S(3)	1.65(5)	C(26)–S(4)	1.81(5)
Fe(1)–C	2.04(av.)	C–C (ring)	1.46(av.)
Bond angles (°)			
S(1)–Pt(1)–S(2)	99.4(4)	S(1)–Pt(1)–S(4)	80.8(4)
S(2)–Pt(1)–S(3)	81.1(4)	S(3)–Pt(1)–S(4)	97.5(4)
S(1)–Pt(1)–S(3)	171.0(4)	S(2)–Pt(1)–S(4)	172.7(4)
C(1)–S(1)–C(21)	105.9(20)	C(11)–S(2)–C(23)	101.2(19)
C(16)–S(3)–C(24)	101.5(22)	C(6)–S(4)–C(26)	96.9(21)
S(1)–C(21)–C(22)	114.6(29)	S(2)–C(23)–C(22)	109.9(26)
S(3)–C(24)–C(25)	121.2(31)	S(4)–C(26)–C(25)	116.4(31)

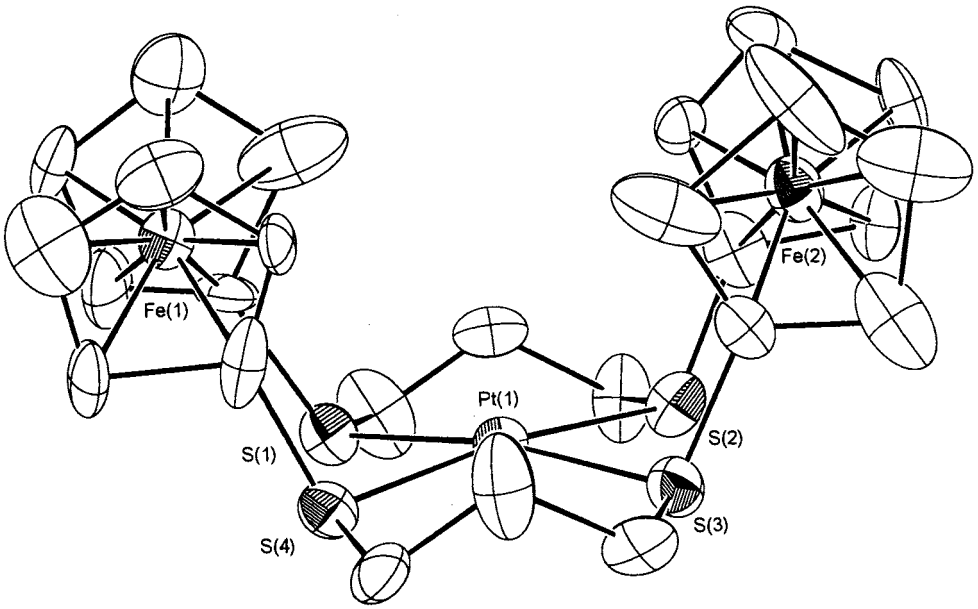

Fig. 4. ORTEP view of the cationic part of **4**.

and Cu(I) complexes (**3**), an irreversible reduction wave and a two-electron quasi-reversible redox wave were observed. The latter wave was assigned to be the redox of the ferrocene moiety in the complexes in terms of the reversibility and the electric current. Their redox potentials are shifted a little to high-potential region compared with that of the free ligand (**1**), implying that the Ag(I) and Cu(I) ions exert only a tiny effect towards the Fe site of the ferrocene moiety. This is coincident with the result deduced from the spectral observation (see above). The Pt(II) complex (**4**) showed an irreversible reduction wave and an irreversible two-electron oxidation wave. In the Pd(II) complex (**5**), the irreversible two waves are similarly observed but the wave in higher potential separated two peaks. The latter wave is probably attributed to the Fe(II)/Fe(III) of the ferrocene moiety of the complexes in comparison with the redox potentials of the reference compounds, e.g. $Fe(CsH_4SMe)_2PdCl_2$ [19] and the Pd(II) complexes of polythiamacrocycles, [*n*]aneS_n ($n = 4$–6) [20], although the wave is irreversible. The oxidation potential of complexes **4** and **5** shifted to more extent to a high-potential region than that of complexes **2** and **3**, suggesting that there is a considerably strong interaction between the Pt(II) or Pd(II) center and the Fe atom of the ferrocene moiety in **4** and **5**. The interaction seems probably due to an inductive or field effect of the Pt(II) or Pd(II) atom through the coordination of the S atom to the metal site as previously described. This is in agreement with the conclusion obtained from the NMR experiment. The observation that the oxidation waves in **5** separated at $+0.63$ and $+0.76$ V may mean that there is a little electronic interaction, probably through the Pd(II) atom between the two ferrocene nuclei, although the essence is uncertain at present.

Table 5
Cyclic voltammetry data (vs. $FcH|FcH^+$)

Compound	E_{pc}	E_{pa}
Ligand (**1**)	—	+0.01
Ag complex (**2**)	−0.88	+0.36
Cu complex (**3**)	−1.15	+0.21[a]
Pt complex (**4**)	−0.99	+0.75
Pd complex (**5**)	−0.45[a]	+0.63
		+0.76
Pd[*n*]aneS_n ($n = 4 \sim 6$)[b]	−0.74 ~ −0.875	—
$Fe(C_5H_4SMe)_2PdCl_2$[c]	−1.00	+0.52

[a] The wave is reversible. The value is $E_{1/2}$; [b] ref. [19]; [c] ref. [18].

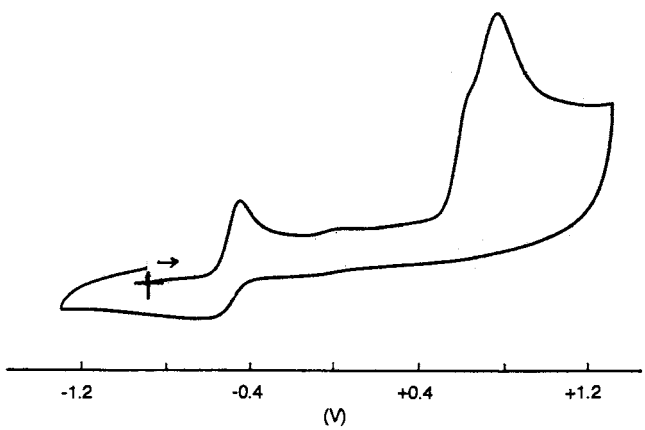

Fig. 5. Cyclic voltammogram of **5**.

3. Experimental

3.1. General

IR spectra were recorded as KBr pellets on a Perkin-Elmer System 2000 spectrometer. NMR spectra were recorded on a Bruker AM400 or ARX400 instrument, using TMS as an internal standard. Electrochemical measurements were by cyclic voltammetry in a solution of 0.1 M $(n\text{-Bu})_4NClO_4$ in CH_3CN or CH_2Cl_2 under nitrogen at 25°C, using a standard three-electrode cell on a BAS CV-27 analyzer. All potentials referenced to $FcH|FcH^+$, which had a potential of $+0.14$ V versus $Ag|AgNO_3$ in this medium. The scan rate was 100 mV s^{-1}. 1,1′-Bis(3-chloropropylthio)ferrocene was prepared according to the literature [11]. All the other chemicals were reagent grade.

3.2. Procedure

3.2.1. 1,5,16,20-Tetrathia[5.5]ferrocenophane (1)

A solution of 1,1′-bis(3-chloropropylthio)ferrocene (3.2 g, 8 mmol) in anhydrous and N_2-saturated THF (50 ml) and EtOH (50 ml) and a solution of disodium 1,1′-ferrocenethiolate prepared from 1,1′-ferrocenethiol (2.0 g, 8 mmol) and NaOH (1.5 g) in anhydrous and N-saturated EtOH (100 ml) were added slowly and at the same rate to anhydrous and refluxing THF (600 ml) under N bubbling for a period of 2.5 h. After the addition had been completed, the mixture was further refluxed for 3.5 h. The solvent was evaporated under reduced pressure. The residue was dissolved in benzene and the mixture was filtered. The filtrate was condensed to a total volume of 50 ml and chilled in the refrigerator. The resulting brown crystals were collected by filtration. The crystals were recrystallized from benzene to give the title compound (**1**) as light brown crystals (1.56 g). The filtrate and the mother liquor of recrystallization were combined and evaporated under reduced pressure. The residue was chromatographed on SiO_2 by elution of hexane/toluene and subsequently toluene to give **1** (0.30 g) along with the dimer of **1** (0.50 g). The yield of **1** was totally 1.86 g (40%). M.p.: 178–180°C. Anal. found: C, 53.61; H, 4.82%. $C_{26}H_{28}S_4Fe_2$ Anal. calc.: C, 53.80; H, 4.86%. ^{1}H-NMR (CD_2Cl_2): δ 1.88 (p, 4H, $J=6.6$ Hz), 3.03 (t, 8H, $J=6.6$ Hz), and 4.29 (dd, 16H, $J=6.0$ and 1.5 Hz). Yield of the dimer: 0.50 g (11%). M.p. 105–108°C Anal. Found: C, 53.88; H, 5.12%. $C_{52}H_{56}S_8Fe_4$ calc.: C, 53.80; H, 4.86%.

3.2.2. The Ag(I) complex of 1 (2)

To a solution of **1** (100 mg, 0.17 mmol) in THF (10 ml) was added a solution of $AgBF_4$ (33 mg, 0.17 mmol) in THF (2 ml). The solution was left to stand in a dark place overnight. The resulting yellow crystals were collected by filtration. Yield: 110 mg (83%). M.p. 220°C (dec.). Found: C, 40.54; H, 3.66%. $C_{26}H_{28}BF_4S_4Fe_2Ag$ calc.: C, 40.29; H, 3.64%. ^{1}H-NMR (CD_2Cl_2): δ 2.02 (m, 4H), 3.06 (t, 8H, $J=5.3$ Hz), 4.51 (dd, 16H, 1.5 and 3.8 Hz).

3.2.3. The Cu(I) complex of 1 (3)

To a solution of **1** (50 mg, 0.085 mmol) in THF (6 ml) was added a solution of $Cu(MeCN)_4ClO_4$ (28 mg, 0.085 mmol) in MeCN (3 ml). The solution was refluxed for 15 min. After the addition of diethylether (3.5 ml), the solution was kept overnight in a refrigerator. The resulting yellow/orange crystals were collected by filtration. Yield: 46 mg (73%). M.p. $\sim$180°C (dec.). Found: C, 42.50; H, 3.75%. $C_{26}H_{28}ClO_4S_4Fe_2Cu$ calc.: C, 42.01; H, 3.80%. ^{1}H-NMR (CD_3NO_2): δ 2.06 (bs, 4H), 3.27 (bs, 8H), 4.52 (bs, 8H), and 4.62 (bs, 8H).

3.2.4. The Pt (II) complex of 1 (4)

A mixture of $(CH_3CN)_2PtCl_2$ (35 mg, 0.10 mmol) and $AgBF_4$ (40 mg, 0.20 mmol) in CH_3CN (10 ml) was refluxed for 2 h. To the mixture was added a solution of **1** (58 mg, 0.10 mmol) in benzene (10 ml) and then the mixture was further refluxed for 2 h. The mixture was filtered and the residue was washed with a small amount of CH_3CN. The filtrate and the washings were combined and evaporated under vacuum. The residue was dissolved in CH_3CN (3 ml) and the solution was filtered. To the filtrate was added acetone (1 ml) and then dry ether drop-wise. The red needles (64 mg, 67%) were obtained. M.p. $>$250°C. Found: C, 33.44; H, 3 07; N, 0 72% $C_{26}H_{28}B_2F_8S_4Fe_2Pt\cdot 1/2CH_3CN$ calc.: C, 33.46; H, 3.17; N, 0.76%. ^{1}H-NMR (CD_3CN, RT): δ 2.41 (quint, 4H, CH_2), 3.08 (br s, 8H, SCH_2), 4.70 (s, 8H, β-H), and 5.24 (s, 8H, α-H). ^{1}H-NMR (CD_3CN, 65°C): δ 2.46 (quint, 4H, CH_2), 3.17 (m, 8H, SCH_2), 4.74 (t, $J=1.9$ Hz, 8H, α-H), and 5.26 (t, $J=1.9$ Hz, RH, α-H). ^{1}H-NMR (CD_3CN, -40°C): δ 2.2–2.5 (m, CH_2), 2.66 (dd, $J=13$ and 2 Hz, *syn*-SCH_2), 2.97 (m, *anti*-SCH_2), 3.09 (t, $J=13$ Hz, *syn*-SCH_2), 3.29 (m, *anti*-SCH_2), 4.50 (s, *anti*-β-H), 4.58 (s, *syn*-β-H), 4.74 (s, *anti*-β'-H), 4.85 (s, *syn*-β'-H), 5.15 (s, *anti*-α-H), 5.22 (s, *syn*-α-H + *anti*-α'-H) and 5.25 (s, *syn*-α-H). This assignment was carried by the H,H-COSY method at the same temperature. ^{13}C-NMR (CD_3CN, RT): δ 25.85 (CH_2), 38.13 (SCH_2), 74.98 (C_5H_4), and 77.69 (C_5H_4).

3.2.5. The Pd(II) complex of 1 (5)

A mixture of $(CH_3CN)_2PdCl_2$ (26 mg, 0.10 mmol) and $AgBF_4$ (40 mg, 0.20 mmol) in CH_3CN (2 ml) was stirred for 1 h at room temperature. To the mixture was added a solution of **1** (58 mg, 0.10 mmol) in benzene (8 ml) and then the mixture was stirred for 30 min. The resulting AgCl was filtered off. The filtrate and the washings were combined and evaporated under vacuum. The residue was dissolved in CH_3CN (3 ml) and

the solution was filtered. To the filtrate was added dry ether (3 ml) and the solution was chilled in a freezer. The green needles (61 mg, 68%) were obtained. M.p. >250°C. Found: C, 37.15; H, 3.54; N, 1.52% $C_{26}H_{28}B_2F_8S_4Fe_2Pd \cdot CH_3CN$ calc.: C, 37.30; H, 3.47; N, 1.55%. ^{1}H-NMR (CD_3CN, RT): δ 2.35 (quint, 4H, CH_2), 2.91 (t, $J=5.5$ Hz, 8H, SCH_2), 4.67 (s, 8H, β-H), and 5.29 (t, $J=1.9$ Hz, 8H, α-H). ^{1}H-NMR (CD_3CN, 35°C): δ 2.35 (quint, 4H, CH_2), 2.93 (t, $J=5.5$ Hz, 8H, SCH_2), 4.68 (t, $J=1.9$ Hz, 8H, β-H), and 5.29 (t, $J=1.9$ Hz, 8H, α-H). ^{1}H-NMR (CD_3CN, -55°C): δ 2.2–2.5 (m, CH_2), 2.58 (bd, $J=13$ Hz, *syn*-SCH_2), 2.71 (m, *anti*-SCH_2), 2.83 (t, $J=13$ Hz, *syn*-SCH_2), 3.12 (m, *anti*-SCH_2), 4.45 (s, *anti*-β-H), 4.55 (s, *syn*-β-H), 4.70 (s, *anti*-β'-H), 4.82 (s, *syn*-β'-H), 5.18 (s, *anti*-α-H), 5.23 (s, *anti*-α'-H), 5.28 (s, *syn*-α-H) and 5.32 (s, *syn*-α-H). ^{13}C-NMR (CD_3CN, RT): δ 26.67 (CH_2), 39.43 (SCH_2), 74.75 (C_5H_4), 78.19 (C_5H_4), and 80.07 (*ipso*-C_5H_4).

4. Structure determination

The crystallographic data are summarized in Table 1 and the position parameters for complexes **1**–**4** are listed in Tables 2–5, respectively.

In complexes **1** and **2**, data collection was performed at room temperature on Mac Science MXC18R diffractometer with graphite monochromated Mo–K_α radiation and an 18-kW rotating anode generator. In complexes **3** and **4**, oscillation and nonscreen Weissenberg photographs were recorded on the imaging plates on Mac Science DIP3000 diffractometer with graphite monochromated Mo–K_α radiation and an 18-kW rotating anode generator. The data reduction and determination of cell parameters were made by the MAC DENZO program system. The structures of complexes **1**–**4** were solved with the SIR method in CRYSTAN-GM (software-package for structure determination) and refined by full-matrix least-squares procedure. Anisotropical refinements for non-hydrogen atom were carried out. All the hydrogen atoms, partially located from differential Fourier map, for complexes **1** and **2** were isotropically refined. In complexes **3** and **4**, no hydrogen was located.

References

[1] S.G. Murray, F.R. Hartley, Chem. Rev. 81 (1981) 365.
[2] S.R. Cooper, Acc. Chem. Res. 21 (1988) 141.
[3] A.J. Blake, M. Schroder, Adv. Inorg. Chem. 35 (1990) 1.
[4] M. Sato, S. Akabori, Trends Org. Chem. 1 (1991) 213.
[5] G.M. Gray, Comments Inorg. Chem. 17 (1995) 95.
[6] M. Sato, S. Tanaka, S. Akabori, Y. Habata, Bull. Chem. Soc. Jpn. 59 (1986) 1515.
[7] M. Sato, R. Suzuki, S. Akabori, Bull. Chem. Soc. Jpn. 59 (1986) 3611.
[8] (a) M. Sato, M. Ratada, S. Nakasima, H. Sano, S. Akabori, J. Chem. Soc. Dalton Trans. (1990) 1979. (b) M. Sato, S. Akabori, M. Ratada, I. Motoyama, H. Sano, Chem. Lett. (1987) 1847.
[9] (a) M. Sato, S. Akabori, Bull. Chem. Soc. Jpn. 62 (1989) 3492. (b) M. Sato, H. Asano, S. Akabori, J. Organomet. Chem. 401 (1991) 363. (c) M. Sato, R. Suzuki, S. Akabori, Chem. Lett. (1987) 2239.
[10] (a) M. Sato, R. Suzuki, H. Asano, M. Sekino, Y. Rawata, Y. Habata, S. Akabori, J. Organomet. Chem. 470 (1994) 263. (b) M. Sato, H. Anano, S. Akabori, J. Organomet. Chem. 452 (1993) 105. (c) M. Sato, H. Asano, R. Suzuki, M. Ratada, S. Akabori, Bull. Chem. Soc. Jpn. 62 (1989) 3828.
[11] M. Sato, S. Tanaka, S. Ebine, S. Akabori, Bull. Chem. Soc. Jpn. 57 (1984) 1929.
[12] G.H. Robinson, S.A. Sangokoya, J. Am. Chem. Soc. 110 (1988) 1494.
[13] R.E. Wolf, J.R. Hartman, J.M.E. Storey, B.-M. Foxman, S.R. Cooper, J. Am. Chem. Soc. 109 (1987) 4328.
[14] (a) P.J. Blower, J.A. Clarkson, S.C. Rawle, et al., Inorg. Chem. 28 (1989) 4040. (b) H.-J. Ruppers, R. Wieghardt, Y.-H. Tsay, C. Krüger, B. Nuber, J. Weiss, Angew. Chem. Int. Ed. Engl. 26 (1987) 575.
[15] R. Alberto, W. Nef, A. Smith, et al., Inorg. Chem. 35 (1966) 3420.
[16] (a) L.L. Diaddario, E.R. Dockal, M.D. Glick, L.A. Ochrymowycz, D.B. Rorabacher, Inorg. Chem. 24 (1985) 356. (b) E.R. Dockal, L.L. Diaddario, M.D. Glick, D.B. Rorabacher, J. Am. Chem. Soc. 99 (1977) 4532.
[17] L.S. Hegedus, T.A. Mulhern, H. Asada, J. Am. Chem. Soc. 108 (1986) 6224.
[18] M. Sato, CASC forum, 17 (1997) 31.
[19] B. McCulloch, D.R. Ward, J.D. Woolins, C.H. Brubaker Jr, Organometallics 4 (1985) 1425.
[20] A.S. Pine, B.J. Howardj, J. Chem. Phys. 84 (1986) 590.